NJC

Cite this: *New J. Chem.*, 2012, **36**, 1187–1200

www.rsc.org/njc

PAPER

Post-polymerisation modification of surface chemical functionality and its effect on protein binding

Cleo Choong,[a] J. S. Foord,[b] Jon-Paul Griffiths,[c] Emily M. Parker,[b] Luo Baiwen,[a] Meghali Bora[a] and Mark G. Moloney*[b]

Received (in Montpellier, France) 2nd January 2012, Accepted 10th February 2012
DOI: 10.1039/c2nj00002d

Derivatisation of polystyrene by carbene insertions followed by diazonium coupling permits the introduction of diverse chemical functionality, providing access to materials with similar bulk properties, but in which surface chemical characteristics are systematically varied across a range of surface polarity, hydration and non-bonding interaction behaviour. Protein binding experiments with bovine serum albumin demonstrate that protein adhesion is dependent upon the identity of the surface chemical group, with *tert*-butyl, hexyl, dimethylamino, amino, and carboxyl modified systems all exhibiting higher levels of binding, while glycol, hydroxyl, and phosphonate give similar or lower levels of binding, relative to the control. This behaviour has been shown to be time dependent, and an approximate trend of protein binding with cheminformatic descriptors %PSA and contact angle was observed.

The control of interfacial properties to modify biocompatibility and cellular adhesion is of immediate relevance in biomaterial and drug delivery devices.[1,2] Previous studies of biomolecule adhesion have shown that proteins bind most strongly to surfaces in the following order: Teflon > siliconized glass > polyvinylchloride > Nylon-6,6, and that hydrophobic proteins (*e.g.* fibrinogen) adsorb to a greater extent than hydrophilic proteins (*e.g.* bovine serum albumin).[3] A similar conclusion was made using variously modified titania.[4] However, poly(ethylene glycol) grafted onto polystyrene has been shown to prevent adsorption of fibrinogen and IgG, as well as the adhesion of *Streptococcus mutans*,[5] and a similar effect has been shown on stainless steel.[6,7] A more detailed examination of fibronectin binding on methyl, hydroxyl, carboxyl and amino-terminated self-assembled monolayers (SAM) on a gold surface has demonstrated that binding affinities of monoclonal antibodies raised against the central cell-binding domain responded to surface chemical functionality in the order: OH > COOH > NH_2 > CH_3, although there were differences in binding preference for α_V and $\alpha_5\beta_1$ integrin.[8] Using phosphotidylcholine and hydroxy terminated polymer brushes, the binding force of bovine serum albumin (BSA) to the modified surface was measured using an AFM cantilever; this was found to vary from 0.1–1.2 nN depending on the layer thickness and surface functionality.[9] A review of the nature of the effects induced by chemical surface functionality describes differences in the behaviour of alkyl, hydroxyl, amine and carboxyl groups[10] and the use of tertiary amine oxide modified surfaces has been shown to resist nonspecific protein adsorption.[11] Very recently the effect of the identity of surface functional groups on gene transfer efficiency has recently been demonstrated.[12] Overall, while these fundamental studies have demonstrated the influence of surface chemical functionality on the interaction of a material with biomolecules, a remaining challenge is the development of methodology suitable for the modification of a diverse range of material types which exploits these phenomena. The significance of precise manipulation of surface properties can be illustrated by the fact that the inability to control surface chemistry has been identified as a key limiting factor in the development of polymer nanofibers as scaffolds for tissue engineering scaffolds, since no single fabrication technique has allowed collective control over structure, material composition, and surface functionality.[13] Surface modification of materials, in such a way that bulk properties are not modified, has been the focus of some attention.[14–16] Although a variety of techniques for surface activation have been developed and applications demonstrated,[17] we have found that an approach based upon the reaction of a wide variety of materials with substituted diaryldiazomethanes, in which a transient carbene is generated thermally or photochemically;[18] it may be used to introduce colour,[19] fluorescence,[20] biocompatibility,[21] biocidal[22] and payload delivery[23] properties to a wide range of substrates,[24] at loadings of the order of 3×10^{14} molecules per cm^2.[25] Our approach, which is illustrated in Fig. 1, creates a chemically activated polymer which can then be further functionalised to the desired surface functionality. The need to

[a] *School of Materials Science and Engineering, Nanyang Technological University, 50 Nanyang Avenue, Singapore 639798*
[b] *Department of Chemistry, Chemistry Research Laboratory, The University of Oxford, 12 Mansfield Road, Oxford, OX1 3TA, UK. E-mail: mark.moloney@chem.ox.ac.uk*
[c] *Oxford Advanced Surfaces Group Plc, Begbroke Centre for Innovation and Enterprise, Oxford University Begbroke Science Park, Sandy Lane, Yarnton, OX5 1PF, UK*

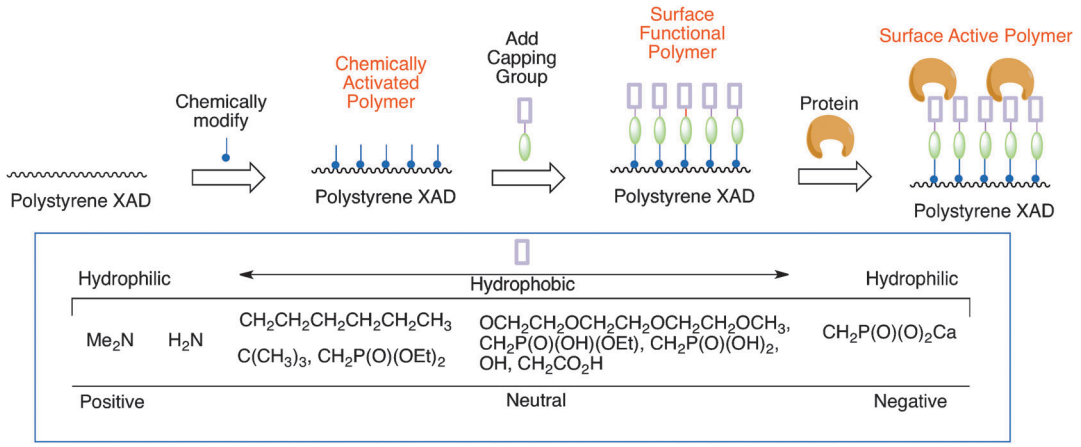

Fig. 1 Diagrammatic representation of the surface modification strategy.

understand the three-way relationship between physical, chemical polymer and functional (*e.g.* antibacterial and biocompatible) polymer properties has been recognised,[26] but of interest to us was the application of the derivatisation process outlined in Fig. 1 to vary surface chemical functionality at controlled loading levels, across a range of hydrophobic/hydrophilic and basic/neutral/acidic groups, to examine the effect of these changes in surface properties on macroscopic properties and protein binding, and where possible to establish correlation of such property changes with modern cheminformatic descriptors of surface chemistry (*vide infra*). We used polystyrene beads as a template, since the pattern of protein adsorption to flat sheets of polymers is reported to be identical to that for adsorption to small polymer particles,[3] and since we have already shown that this approach is equally applicable to other substrates,[19,24] the data obtained from this study would be expected to be generally applicable.

Results and discussion

In order to allow rapid access to functionally variable polystyrenes, we adapted our previously published approach for surface modification using diarylcarbenes and its subsequent modification by diazonium salt coupling;[25] this is a convenient and efficient method for the introduction of diverse chemical functionality onto a material substrate. Thus, bromomethylbenzophenone **1** was treated with 2-*N*-ethylanilinoethanol to give ether **2a**, which was converted to the hydrazone **2b** (as a mixture of *syn*-/*anti*-diastereomers) and then oxidised to the diazo compound **2c**; the success of the latter reaction was immediately evident, as the product is a dark pink oil (Scheme 1). This material is not stable to silica chromatography and is light sensitive, but can be easily stored for extended periods at 0 °C or lower. Dispersion of this material on polystyrene XAD in an ether solution followed by careful solvent removal and heating to 120 °C gave decolourisation, leading to the modified polystyrene **3**; decolourisation is consistent with loss of the diazo function, and conversion to the reactive carbene intermediate prior to surface reaction. This material was then treated with diazonium salts **4a–i**, themselves derived from the required substituted aniline by reaction with isopentyl nitrite (the presence of the desired diazonium salt was confirmed by application of the H-acid test (Scheme 2), giving an intense purple colour when the diazonium function was correctly formed). This two-step coupling process led to modified polystyrene polymers **5a–c** and **5e–j**, possessing terminal *tert*-butyl, hexyl, iodo, phenyl, glycol, hydroxyl, phosphonate diester, amine, and carboxylate groups respectively. Further manipulation of amino **5i** and phosphonate **5h** gave polymers **5d** and **5k–m** terminating with dimethylamino, phosphonate monoester, phosphonic acid and calcium phosphonate substituents, respectively. Aside from the inherent flexibility of this approach, an additional advantage is that successful diazonium coupling to give the extended diazo-containing chromophore on modified polymers **5a–m** as shown in Scheme 1 enables immediate visual indication by the generation usually of intense red or orange, or less frequently, yellow colours (Table 1). This modification could be achieved without physical disruption to the spherical surface as evident from the SEM images of representative samples (unmodified polystyrenes, **5a**, **5d**, **5g**; (Fig. 2)), although it also became apparent that modified samples could become brittle and excessive abrasion led to onion-peel cleavage of the spheres. Polystyrenes **3** and **4d** (R = H), with no peripheral chemical functionality, provide useful controls, relative to the other samples.

Detailed analysis of modified polymers **5a–m** after extensive washing was able to confirm successful chemical modification (Table 1). Thus, the presence of the expected functionality was readily demonstrated by a combination of ATR FTIR and XPS analysis, and combustion analysis allowed a direct estimation of the surface loading levels. Unmodified polystyrene has strong absorbances at 2931, 1657, 1604, 1446, 1220, 990 and 902 cm^{-1},[27] and ATR-IR analysis of modified polymers provided direct evidence for the surface modification with the expected functional groups; unfortunately, the diazo absorbance in the 1400–1500 cm^{-1} region tends not to be well-defined and is often inactive, and was not observed in any of the materials **5a–m**.[28] However, bands of interest such as 3400 (O–H), 1723 (C(O)OH), 1600–1585 (aromatic C–C stretch), 1276 (P═O), 1218 (P═O), 1275–1220 (aryl C–O–C stretch), 1075–1020 (alkyl C–O–C stretch), 1062–1081 cm^{-1} (P–O–C), all of which are associated with the expected functional groups introduced at the polymer surface, were observed (Table 1). Combustion analysis for the nitrogen content of the modified polymers **5a–m** also confirmed the presence of nitrogen and enabled determination of the loading stoichiometry of the polymer. The presence of nitrogen is diagnostic for a successful outcome of the two steps leading to derivatised polymers **3** and **5a–m**.[21,25]

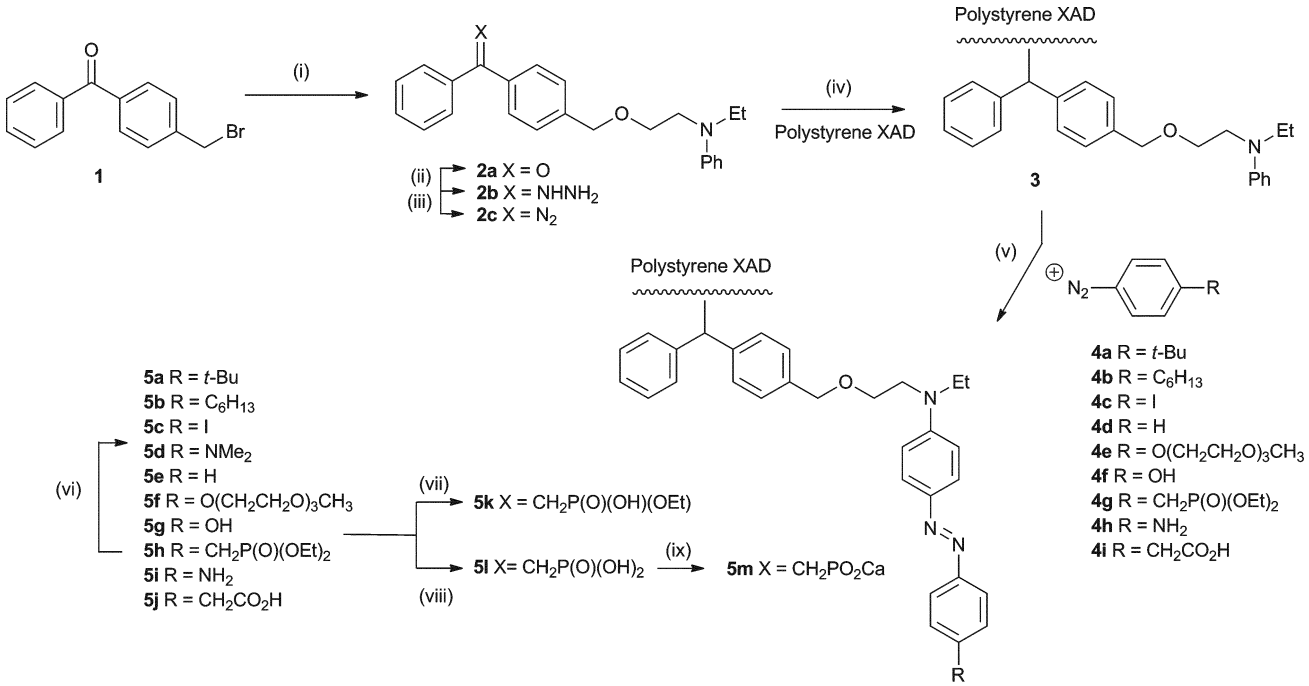

Conditions: i) PhN(Et)CH_2CH_2OH, NaH, THF, RT, 72 h (70-77%); ii) NH_2NH_2, H_2O, EtOH, reflux, 17 h (51-95%); iii) MnO_2, KOH, MeOH, RT, 3 h (62-88%); iv) 120°C; v) soak in EtOH salt solution, 18 h; vi) stir for 18 h in solution of MeI in EtOH vii) soak in 5% aq. NaOH, 18 h; viii) soak in 1M HCl, 18 h ; ix) wash with 10% aq. $Ca(OH)_2$. Diazonium salts **4a-i** were synthesised from corresponding amines by reaction with isopentyl nitrite and HBF_4 in EtOH at 0ºC, 1 h.

Scheme 1

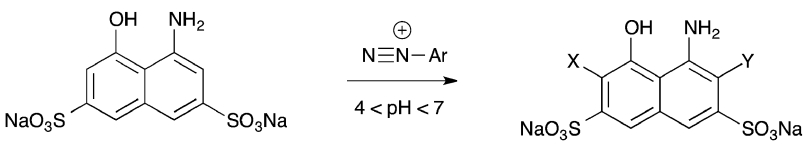

X, Y = H, N=NAr

Scheme 2

Typical surface loading levels were in the range 0.04–0.36 mmol g^{-1} and assuming the manufacturer's value for the surface area of the polymer (725 m^2 g^{-1}), this corresponded to 0.31–2.97 × 10^{13} molecules cm^{-2} (Table 1). These values are comparable to the loading levels in a related polystyrene system modified with a dimethoxydiarylmethylene system, determined to be 0.04–0.18 mmol g^{-1} or 2–15 × 10^{12} molecules cm^{-2},[25] and consistent with other modified polystyrene systems.[29] The presence of nitrogen species in polystyrene samples **3** and **5a–m** was further confirmed from XPS analysis, in which N1s signals at binding energies (eV) of 397.7, 398.5, 399.2, 401.6 and 402.7 eV were observed, with the observed N/C ratios comparing well with the expected values, assuming the formation of a uniform monolayer of benzhydryl units of the indicated molecular formula for modified polymers **5a–m** (Scheme 1 and Table 1). Moreover, the presence of phosphorus in samples **5h**, **k–l** was confirmed by combustion analysis (Table 2), and comparison of the P *versus* N content values permitted estimation of the efficiency of the final diazonium step in Scheme 1 to be typically in the range of 72–76%. When blank polystyrene is treated directly with the diazonium phosphonate **4g** followed by hydrolysis under acid or alkaline conditions, the coupling efficiency is found to be 53 and 28% respectively; this drop of efficiency under alkaline conditions may be due to the hydrolysis conditions eroding the surface of the beads. These data may be further considered in terms of the density of surface coverage of the layer: the limiting area (A_o) for monolayer formation of benzene is 0.24 nm^2 per molecule and for substituted anthracenes it is 0.45–0.48 nm^2 per molecule,[30] and assuming a limiting area of 1.71 nm^2 per molecule as calculated using Chemicalize[31] for the cross-sectional area of a typical surface modifying molecule, it is possible to estimate the surface area coverage as being in the range 6–25% of the total surface area (Table 1). Expressed in a different way, the ratio of unmodified to modified sites (N) on the polymer surface has been calculated to be in the range of 50–200; this loading density is better than the values in a related system prepared by dimethoxydiarylmethylene insertion into polystyrene.[22,25]

To confirm that the chemical modification resulting from the application of the process in Scheme 1 only results in surface modification, without degradation of the bulk of the material, DSC and TGA analysis were performed (see Table 1); the measurable inflection temperature was found to be unaffected in all the samples relative to unmodified polystyrene XAD, with

Table 1 Characterisation data for polymers **5** modified according to Scheme 1

Material and appearance	Combustion analysis %N mmol g^{-1} molecules cm^{-2}[a] % Area covered[b] N[c]	ATR IR/cm^{-1}	XPS N/C found[e] (N/C expected[d]) N[c]	DSC T/°C
Polystyrene XAD-4[f]				
	—	2931, 1657, 1604, 1446, 1220, 990, 902	—	104.4
3 (Carbene modified)	0.25 0.179 1.48×10^{13} 25.4 50	1601, 1511, 1252, 1169, 1090	0.056 (0.040) 2	104.6
				
5a R = *t*-Bu	0.26 0.062 5.14×10^{12} 8.8 150	1603, 1513, 1354, 1252, 1178, 1085	0.086 (0.048) 4	103.8
				
5b R = C_6H_{13}	0.28 0.067 5.54×10^{12} 9.5 138	1326, 1602, 1080	0.020 (0.081) 17	104.4
				
5c R = I	1.5 0.357 2.97×10^{13} 20.4 51	1601, 1377, 1286, 1075, 547	0.041 (0.097) 5	118.8
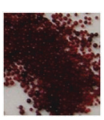				
5d R = NMe_2	0.21 0.038 3.12×10^{12} 5.3 251	1601, 1511, 1351, 1170, 1086	0.12 (0.042) 9	103.9
				
5e R = H	0.7 0.167 1.38×10^{13} 23.7 52	1602, 1511, 1316, 1195, 1092	0.074 (0.097) 2	104.6
				
5f R = $O(CH_2CH_2O)_3CH_3$	0.52 0.124 1.03×10^{13} 17.6 71	1603, 1511, 1362, 1252, 1085	0.044 (0.079) 19	104.6
				
5g R = OH	0.24 0.057 4.75×10^{12} 8.1 161	3400, 1603, 1512, 1252, 1169, 1086	0.031 (0.097) 11	103.2
				

Table 1 (*continued*)

Material and appearance	Combination analysis %N mmol g^{-1} molecules cm^{-2a} % Area covered[b] N[c]	ATR IR/cm^{-1}	XPS N/C found[e] (N/C expected[d]) N[c]	DSC T/°C
5h R = $CH_2P(O)(OEt)_2$ 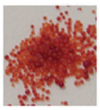	0.34 0.121 1.01×10^{13} 17.2 72	1602, 1276, 1217, 1191, 1062	0.038 (0.083) 8	103.6
5i R = NH_2 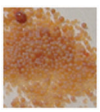	0.26 0.046 3.86×10^{12} 6.6 202	3404, 3280, 1602, 1328, 1217, 1062	0.026 (0.129) 33	104.4
5j R = CH_2COOH 	0.22 0.052 4.35×10^{12} 7.4 178	3020, 1793, 1723, 1602, 1329, 1085	0.041 (0.091) 7	104.3
5k R = $CH_2P(O)(OEt)(OH)$ 	0.63 0.150 1.25×10^{13} 21.3 58	2606, 1602, 1298, 1081, 1071	0.033 (0.088) 8	105.0
5l R = $CH_2P(O)(OH)_2$ 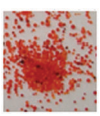	0.61 0.145 1.21×10^{13} 20.6 60	2601, 1602, 1352, 1276, 1251, 1170, 1083, 1018	0.050 (0.094) 3	104.9
5m R = $CH_2P(O)(O)_2Ca$ 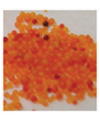	0.32 0.076 6.33×10^{12} 10.8 120	2625, 1601, 1511, 1252, 1170, 1084	0.039 (0.094) 6	103.9

[a] Calculated on the basis of 725 $m^2 g^{-1}$. [b] A limiting area of 1.71 nm^2 per molecule is assumed as calculated using Chemicalize (www.chemicalize.com). [c] *N* is the ratio of unmodified sites to modified sites calculated using the combustion analysis or XPS data. [d] Expected values calculated from molecular formulae assuming a surface monolayer of carbene insertion product. [e] Ratio taken from nitrogen and carbon counts in a survey spectrum. [f] For a thorough list of surface properties of unmodified polystyrene, see http://www.accudynetest.com/polymer_charts.html.

values of 103–105 °C being observed. This transition probably corresponds to the T_g of low levels of residual non-cross-linked material (AMBERLITE™ XAD™4 is a polymeric adsorbent based on highly cross-linked, macroreticular polystyrene (http://www.dow.com/products)),[32] since polystyrene without any additives (M_w=374 000, M_w/Mn=2.5) has been reported to have T_g-values in the range 107 °C ± 2 K.[33] The influence of polystyrene blending on T_g has been investigated[34] and cross-linking of polystyrene has been reported to increase the T_g value from 98 °C to 125 °C.[35] It was found that the TGA degradation temperature (all samples have degradation temperatures between 470–476 °C) was unaffected after surface modification.

With this library of diversely functionalised polystyrenes **3** and **5a–m** in hand, an assessment of the changes to macroscopic behaviour was made. In order to permit a more quantitative analysis of the outcomes of this work, an initial calculation of the value for several molecular characterisation parameters which are increasingly used to guide the drug discovery process,[36] including polarisability, calculated molecular refractivity (CMR), log *P*, polar surface area (PSA), molecular surface area (MSA) and molecular volume, was made using Marvin (www.chemaxon.org, accessed *via* chemicalize.org),[31] and the relevant data are included in Table 3 (columns 2–7). Polarisability is a measure of induced charge resulting from polar

Table 2 Combustion analysis for P and N for selected substrates

Material	Functionality	Measured %P/ mmol g^{-1}	Measured %N/ mmol g^{-1}	Expected mmol g^{-1} I or P[a]	% Efficiency for diazonium coupling[b]
5k	R = $CH_2P(O)(OH)(OEt)$	0.11 (0.036)	0.63 (0.150)	0.050	72
5l	R = $CH_2P(O)(OH)_2$	0.17 (0.055)	0.61 (0.145)	0.048	75
5m	R = $CH_2P(O)O_2Ca$	0.06 (0.019)	0.49 (0.076)	0.025	76

[a] Expected %P = measured %N/3. [b] Efficiency = actual P/expected P.

interactions, and is calculated by the method of Miller and Savchik.[37] CMR, calculated using the method of Ghose and Crippen,[38,39] correlates molecular refractivity with the molecular volume and therefore London dispersive forces, which are important in molecular interactions. *c* log *P* is the octanol/water partition coefficient, calculated using the method of Ghose *et al.*,[39] and is a measure of the lipophilicity of a compound. The polar surface area parameter (PSA), which correlates the presence of polar atoms with membrane permeability and therefore gives an indication of drug transport properties,[40] has been reported to have an optimal value of 70 < PSA < 120 Å^2 for a non-CNS orally absorbable drug.[41] MSA is the van der Waals molecular surface area, and is calculated using the method of Ferrara *et al.*[42] Although strictly applicable to molecules in solution, given the length of the linking tether which permits a high degree of freedom in the modified polymers **5a–m**, this analysis nonetheless provides a useful measure of the types of surface property likely to impact on macroscopic behaviour of the modified polystyrene beads. In this analysis, the steadily decreasing lipophilic and increasing hydrophilic character of modified materials **5a–m** was confirmed from their decreasing *c* log *P* values and increasing %PSA values (Table 3). The calculated van der Waals molecular surface area of the modifying surface functionality is in the range 870–1170 Å^2,[42] the difference arising from the various lengths of the functional group R of the common structural skeleton in **5a–m** (Table 3 and Scheme 1). This is also reflected in the calculated molecular volume, which is in the range 540–700 Å^3 (Table 3).

With this data in hand, an analysis of the macroscopic properties of modified polystyrenes was made; thus, water contact angle and Zeta potential (ξ) were measured. Contact angle behaviour can be complex,[43–46] and polystyrene has been thoroughly studied;[47,48] surface functionalisation of polystyrene with polar groups and poly-L-lysine has been shown to lead to the significant reduction of contact angle.[5,48,49] In the case of the modified polystyrene beads prepared herein, the curved nature of the beads required special analysis for contact angle, and this was achieved by using "floating" contact angle measurements, using the literature method.[50] For these measurements, the polystyrene microspheres were randomly chosen from each sample group and carefully placed on the surface of a (deionized) water droplet contained on a clean glass slide. The wetting behaviour (*i.e.* contact angle at the microparticle/water interface) was then measured in side elevation, and the data are given in Table 3. This investigation indicated that most materials exhibited

Table 3 Polymer characterisation and cheminformatic data[a]

Polymer	*c* log *P*	Polarisability	Molecular refractivity	Molecular surface area	% Polar surface area	Volume/ Å^3	Contact angle/°	Surface tension (solid–liquid interface)/mJ m^{-2}	Zeta potential/ mV	Protein adsorption (mg protein/mg polymer)	Surface loading[b]/ mmol g^{-1}	Protein adsorption per mmol g^{-1} of polymer loading
Polystyrene XAD-4	—	—	—	—	—	—	52	85.8	−27.8	0.027	0	N/A
3 (carbene)	8.6	55.7	114.9	743.6	1.7	453.0	37	100.1	−24.9	0.036	0.18	0.20
5a (R = *t*-Bu)	12.6	74.2	197.9	1009.5	3.7	610.4	59	79.4	17.9	0.020	0.062	0.32
5b (R = Hexyl)	13.8	77.9	207.3	1006.0	3.7	644.0	55	83.8	12.4	0.037	0.067	0.55
5c (R = D	12.0	71.6	192.6	906.2	4.1	565.5	59	79.5	16.0	0.045	0.36	0.13
5d (R = NMe_2)	11.1	73.8	193.7	965.8	4.2	587.7	59	78.9	16.0	0.015	0.038	0.40
5e (R = H)	11.0	66.9	179.2	870.07	4.3	540.8	64	74.0	13.8	—	0.17	—
5f (R = Glycol)	10.8	82.4	218.9	1164.6	6.4	697.5	43	95.2	14.6	0.031	0.12	0.25
5g (R = OH)	10.7	67.4	181.2	892.2	6.4	549.9	53	86.0	12.4	0.025	0.057	0.44
5h (R = $P(O)(OEt)_2$)	11.4	80.6	213.6	1119.1	6.5	672.5	49	89.8	16.6	0.033	0.12	0.27
5i (R = NH_2)	10.2	68.0	183.9	896.3	7.1	551.9	51	87.8	10.6	0.030	0.046	0.65
5j (R = CH_2COOH)	10.4	71.0	190.5	950.9	7.8	586.7	50	88.8	10.8	0.036	0.052	0.68
5k (R = P(O)(OEt)OH)	9.5	76.70	204.3	1049.0	8.0	636.2	50	88.8	8.2	0.095	0.15	0.63
5l (R = $P(O)(OH)_2$)	8.5	72.7	195.1	980.1	9.7	601.3	73	63.3	11.5	0.038	0.15	0.26
5m (R = $P(O)O_2Ca$	8.5	72.5	192.8	975.6	10.3	596.5	73	63.3	−13.2	0.045	0.076	0.65

[a] Polarisability, molecular refractivity, molecular surface area, % polar surface area, and volume (A^3) all calculated using Marvin (www.chemaxon.org). [b] Taken from Table 1. [c] Protein adsorption per mmol g^{-1} of polymer loading = Protein adsorption (mg protein/mg polymer) ÷ Surface loading (mmol g^{-1}).

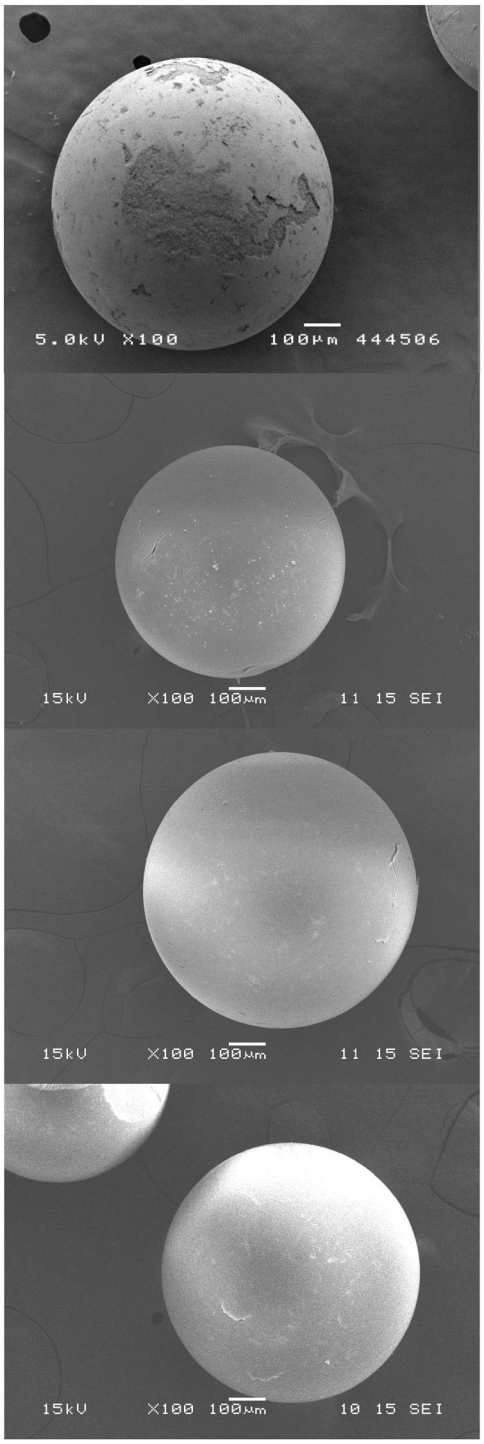

Fig. 2 SEM images of modified beads: (i) unmodified polystyrene XAD; (ii) **5a**; (iii) **5d**; (iv) **5g**.

altered contact angle relative to unmodified polymer (52°), with increasing contact angle broadly correlating with increasing *c* log *P* (columns 2 and 8, Table 3 and Fig. 3(a)). However, although no meaningful correlation of polarisability, CMR or %PSA with contact angle could be observed, more polar groups generally gave a material which was more hydrophilic, as might be expected (*e.g.* polymers **5l,m**); this outcome is consistent with a qualitative classification scheme for hydrophilic and hydrophobic biomaterial surfaces proposed by Hoffman 25 years ago.[51] Surface tension values were derived from contact angle by use of methodology reported by Boury *et al.*[44,52] Measurement of the Zeta potential (ξ) of modified particles was also made, but was complicated by difficulties with the dispersion of the particles. However, by using an acetone-deionised water mixture (11% acetone-deionised water with pH adjusted to ~7.2), suitable particle dispersion could be achieved. The data obtained (column 7, Table 3 and Fig. 3(b) and(c)) indicated that surface modification led to significant alteration of surface charge in most cases relative to unmodified polystyrene XAD (−27.8 mV); a broad correlation of Zeta potential with %PSA and *c* log *P* was observed, since increasing %PSA led to decreasing Zeta potential, while increasing *c* log *P* gave increasing Zeta potential. In sum, more polar chemical functionality at the surface is reflected in more hydrophilic macroscopic behaviour at the surface interface, as might be expected, and since the impact of changes of Zeta potential on protein (BSA) adsorption on hydroxyapatite has been demonstrated, similar effects might be anticipated with these modified polystyrenes.[53]

In order to assess the effect of these polymer modifications on protein adsorption, bovine serum albumin (BSA) adsorption, chosen as a readily available protein, after 3 hours of incubation was measured; adsorption was assessed by isolating and washing the incubated beads, followed by a spectrophotometric assay of the protein after desorption using sodium dodecyl sulfate solution. The raw protein binding values are listed in Table 3 (column 11), but correction of these values by allowance for the differing functional group loading levels permitted calculation of adjusted protein adsorption (mg protein/mg polymer per mmol g^{-1} of polymer chemical functionality loading, Table 3, column 13). No significant correlation of protein adsorption with several parameters could be observed, although increasing values of contact angle, surface tension, and %PSA, and decreasing Zeta potential were generally reflected in higher levels of adjusted protein adsorption (Fig. 4a–d). Neither was correlation of molecular volume with adjusted protein adsorption observed (Fig. 4e). This cheminformatic analysis, based as it is on various measures of polarity or hydrophobicity/philicity, does not allow for the known binding of specific chemical functional groups to BSA. In fact, plasma protein binding is well studied[54,55] and it has been reported that small molecules, in particular carboxylate, halogens and alkyl groups, strongly bind to HSA-3A while anilines do so only weakly.[56–59] Similarly, BSA is known to exhibit strong binding behaviour with carboxylic acids, with binding activity increasing with increasing pK_a.[60] A study of the adsorption of bovine serum albumin (BSA) at the free water interface using surface tension measurements has been reported, parameterised using only bulk diffusion[61] and that chemical functionality can reduce the binding of BSA and fibrinogen has been demonstrated by the incorporation of poly(L-lysine)-*g*-poly(ethylene glycol) layers onto metal oxide surfaces.[62] Therefore, of interest are the high binding values for the hexyl, amine, carboxyl, phosphonate mono ester and calcium phosphonate salt terminated systems **5b,i,j,k,m**; conversely, the weak binding of iodo **5c**, dimethylamino **5d**, glycol **5f**, diethyl phosphate **5h** and phosphonate **5l** is also noteworthy. The weak binding of modified system **5f** is consistent with the known low protein binding behaviour of PEG coatings, as a result of the formation of a tightly bound water layer.[6] Thus, the

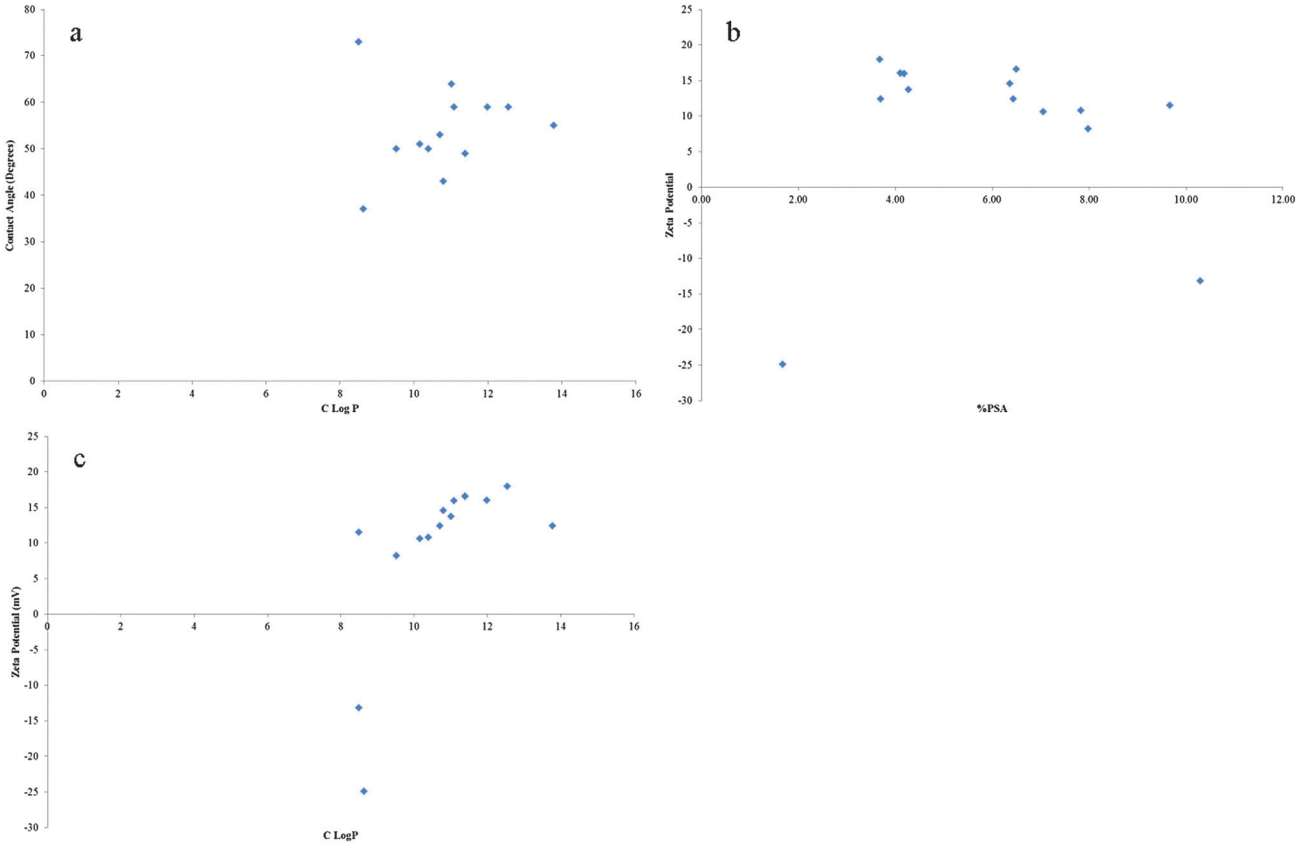

Fig. 3 Plots of (a) contact angle *versus* *c* log *P*; (b) Zeta potential *versus* %PSA; and (c) Zeta potential *versus* *c* log *P* for modified polymers **5a–m** (data from Table 3).

behaviour of the modified polymers **5a–m** is broadly consistent with the known functional group binding behaviour of serum albumins, but noteworthy differences are amine **5i** and phosphonate **5l**.

More detailed analysis in which time course measurements of the levels of protein adsorption were made at 1, 3, 6, 12 and 24 h incubation times was performed; in this case, adsorption was assessed by the spectrophotometric assay of aliquots of the supernatant protein solution taken at various time points, and calculation of adsorbed protein by difference. The resulting data are summarised in Table 4 and Fig. 5(a) and 5(b). The former gives raw data and the latter, protein adsorption adjusted with surface loading density (data taken from Tables 1 and 3). It is immediately apparent that functional group and time variant behaviour is observed; thus, *tert*-butyl **5a**, hexyl **5b**, dimethylamine **5d**, amine **5i**, and carboxyl **5j** all exhibited levels of protein adsorption which were 2–3 times higher relative to the aniline-modified polymer **3** control, but that glycol **5f**, hydroxyl **5g**, and phosphonate diethyl ester **5h** were similar to or gave only slightly increased binding relative to the control aniline **3**; this outcome is similar to that observed in the single point time measurements, the data for which are given in Table 3. However, most samples exhibited complex protein binding behaviour in the time domain, and some systems displayed either increasing or decreasing protein binding over time (*e.g.* hexyl **5b** and hydroxyl **5g** respectively). Initial binding broadly linearly correlated with contact angle at $t = 3$ h (Fig. 6(a)) with an R^2 value of 0.7425, and this trend was preserved, albeit more weakly, at $t = 12$ h ($R^2 = 0.5168$), but lost at $t = 24$ h ($R^2 = 0.3641$), consistent with surface saturation of hydration and/or protein binding over this time period. Of interest is the increase in the slope of the lines of best fit for correlations of contact angle and protein binding (Fig. 6(a), (c) and (e)) as the system approaches saturation, and that in Fig. 6(a), (c) and (e), there are two groups of chemical function, the more polar grouping at the top, for which protein binding is preserved over the time course of the experiment, and the non-polar at the bottom, for which protein binding decreases over time. Within the time frame of the experiment, the aniline **3**, glycol **5f** and hydroxy **5g** modified surfaces exhibit similar behaviour for protein binding, and this may be due to the presence of a significant hydration layer, which is not present in the hydrophobic modifications containing *tert*-butyl and hexyl groups **5a,b**. By 24 hours, two distinctive groups have formed; the low-binding group which includes the aniline, glycol, hydroxy and phosphonate diester modified polymers, and the high-binding group which is made up of the more hydrophobic alkyl terminated polymers hexyl and *tert*-butyl as well as dimethyl amine, amine and acid terminated groups. The alkyl terminated polymers will have low (+) ΔG dehydration values and would be expected to bind proteins using van der Waals London forces in a separate binding site to that which supports the more polar surfaces. *tert*-Butyl and dimethylamine modified surfaces have very similar adsorption levels, and this may reflect similar steric interactions with the protein binding site. The acid and amine are the two that do not fit in with this group

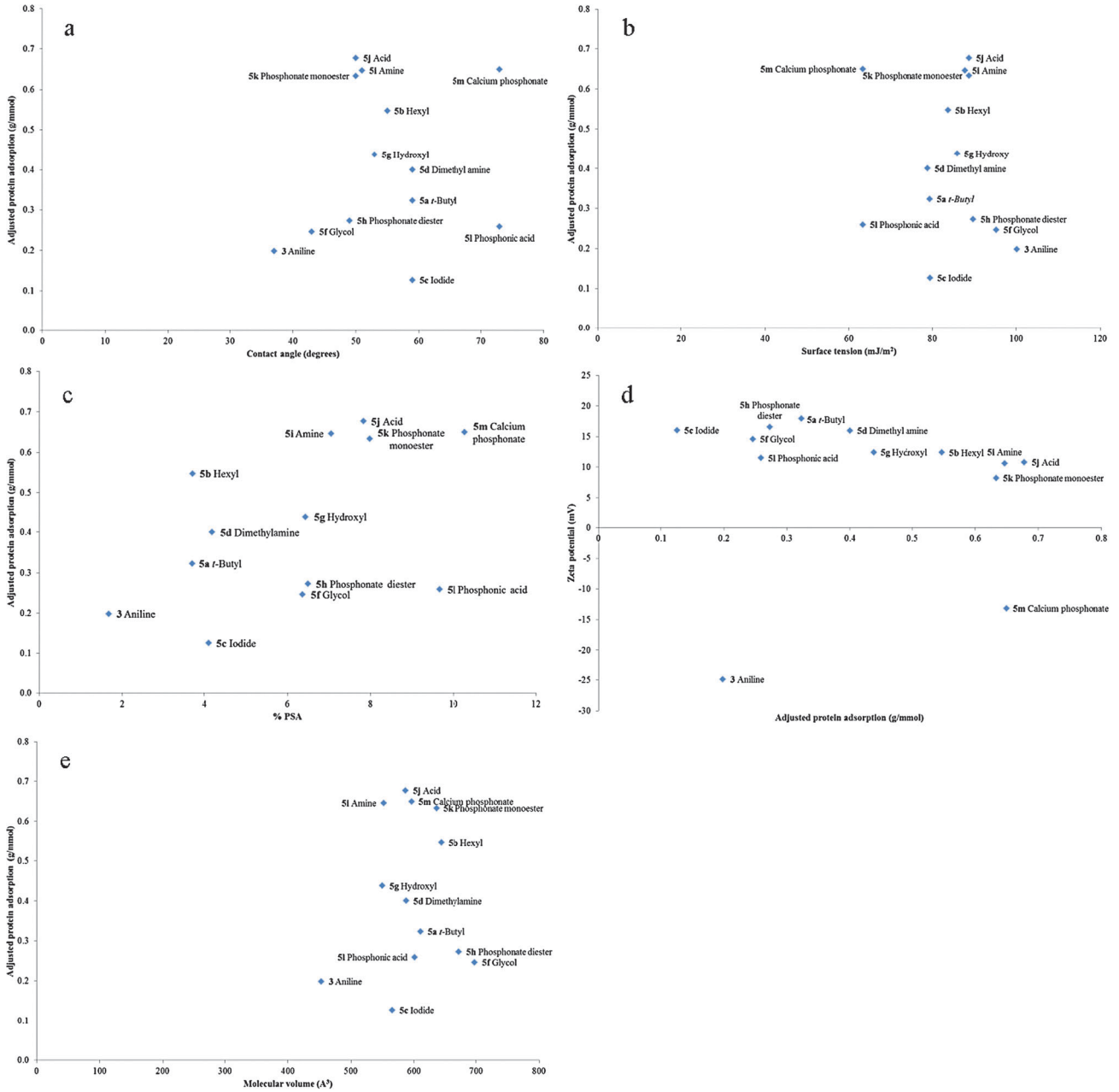

Fig. 4 Plots of (a) contact angle *versus* adjusted protein adsorption; (b) adjusted protein adsorption *versus* surface tension; (c) %PSA *versus* adjusted protein adsorption; and (d) molecular volume *versus* adjusted protein adsorption; and (e) adjusted protein adsorption *versus* zeta potential for modified polymers **5a–m** (data from Table 3).

Table 4 Protein binding data for selected modified polystyrenes

	Normalized %protein adsorption (%/mmol g^{-1})				
Samples	1/h	3/h	6/h	12/h	24/h
3 Carbene modified	42.3	32.3	26.6	22.7	33.7
5a R = *t*-Bu	121.1	82.0	136.7	126.8	119.2
5b R = C_6H_{13}	88.1	92.1	113.8	137.7	144.0
5d R = NMe_2	113.6	169.8	207.0	157.4	115.6
5f R = $O(CH_2CH_2O)_3CH_3$	60.47	61.9	54.37	38.5	38.8
5g (OH)	104.5	33.6	98.97	43.74	44.6
5h R = $CH_2P(O)(OEt)_2$	72.6	27.8	86.1	91.19	53.5
5i R = NH_2	106.8	82.1	169.0	117.5	132.6
5j R = CH_2COOH	117.4	148.7	194.0	168.9	165.2

in terms of shape and hydrophobicity; this is likely to reflect their known binding to alternative binding sites on BSA *via* electrostatic interactions. Noh and Vogler *et al.* [63,64] break the Gibbs energy of protein adsorption down into three different components: (i) ΔG hydrophobic effect, which can be described as the energy gained as the protein comes out of solution and the water forms hydrogen bonds with itself, and this can be assumed to be constant; (ii) ΔG dehydration, which is the energy required to displace the water adsorbed onto the polymer surface (as the hydration of the surface increases protein adsorption decreases due to the protein having to dispel the hydrated layer in order to adsorb onto the surface); (iii) ΔG interaction, which considers the affinity of the protein for the surface and energy gained in forming

(a) Raw Data

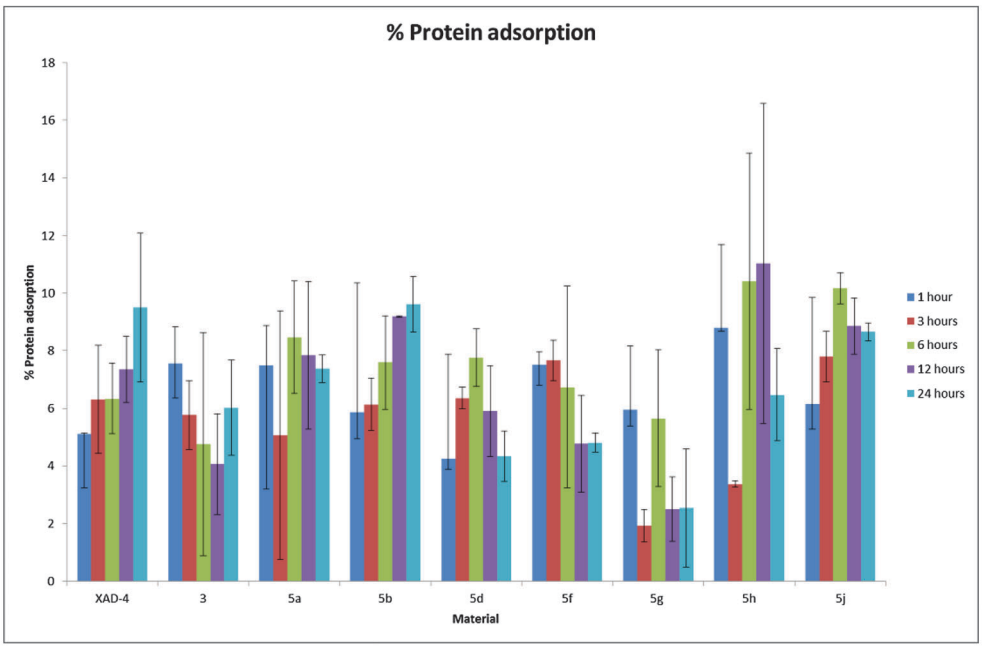

(b) Adjusted for Surface Functional Loading

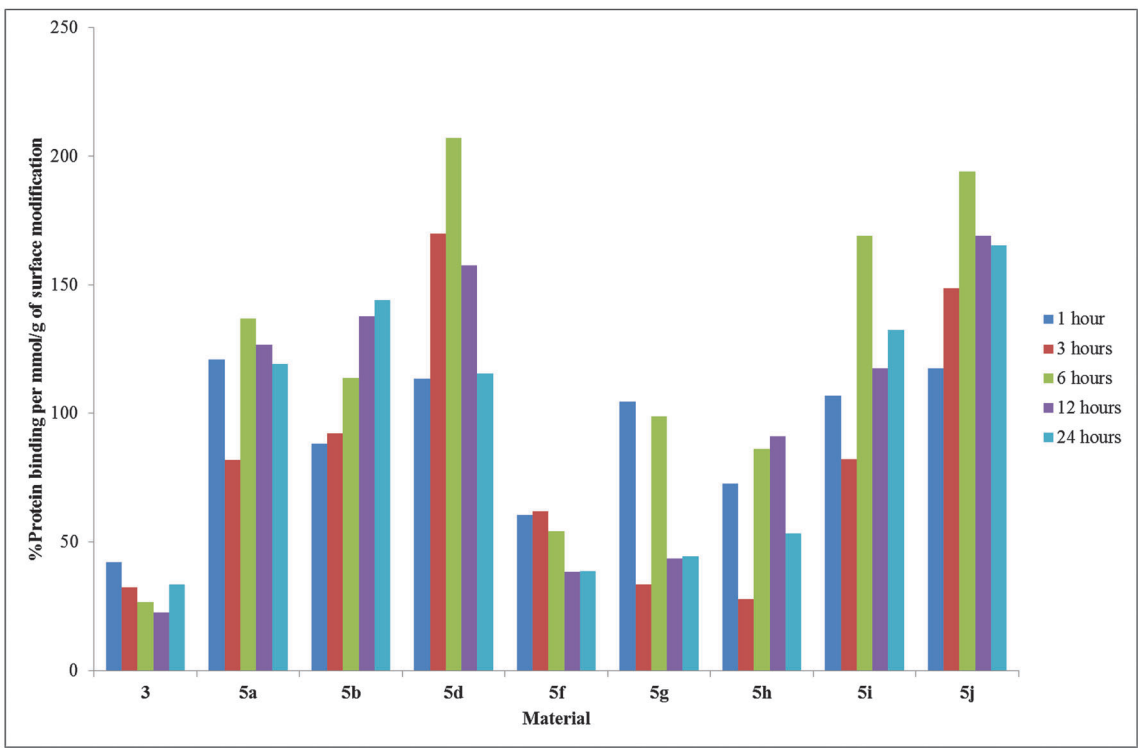

Fig. 5 Bar chart illustrating normalised %protein adsorption by functional group.

the protein surface interactions by electrostatic, hydrogen bonding or van der Waals forces. The latter may be more important over time and may explain why the amine, acid and hydroxyl materials bind more protein initially than other functional groups.

On the other hand, the data in Fig. 6(b) and (d), which correlate protein binding with cheminformatic parameters included in Table 3, are best accounted with two trends, enclosed within the indicated circles, one for non-polar and the other for polar groups defined by their %PSA, with the less polar surfaces between 1.7–4.2% and the more polar between 6.4–7.8%, and this may be indicative of binding at the two known binding pockets of BSA.[54–60] By 24 hours

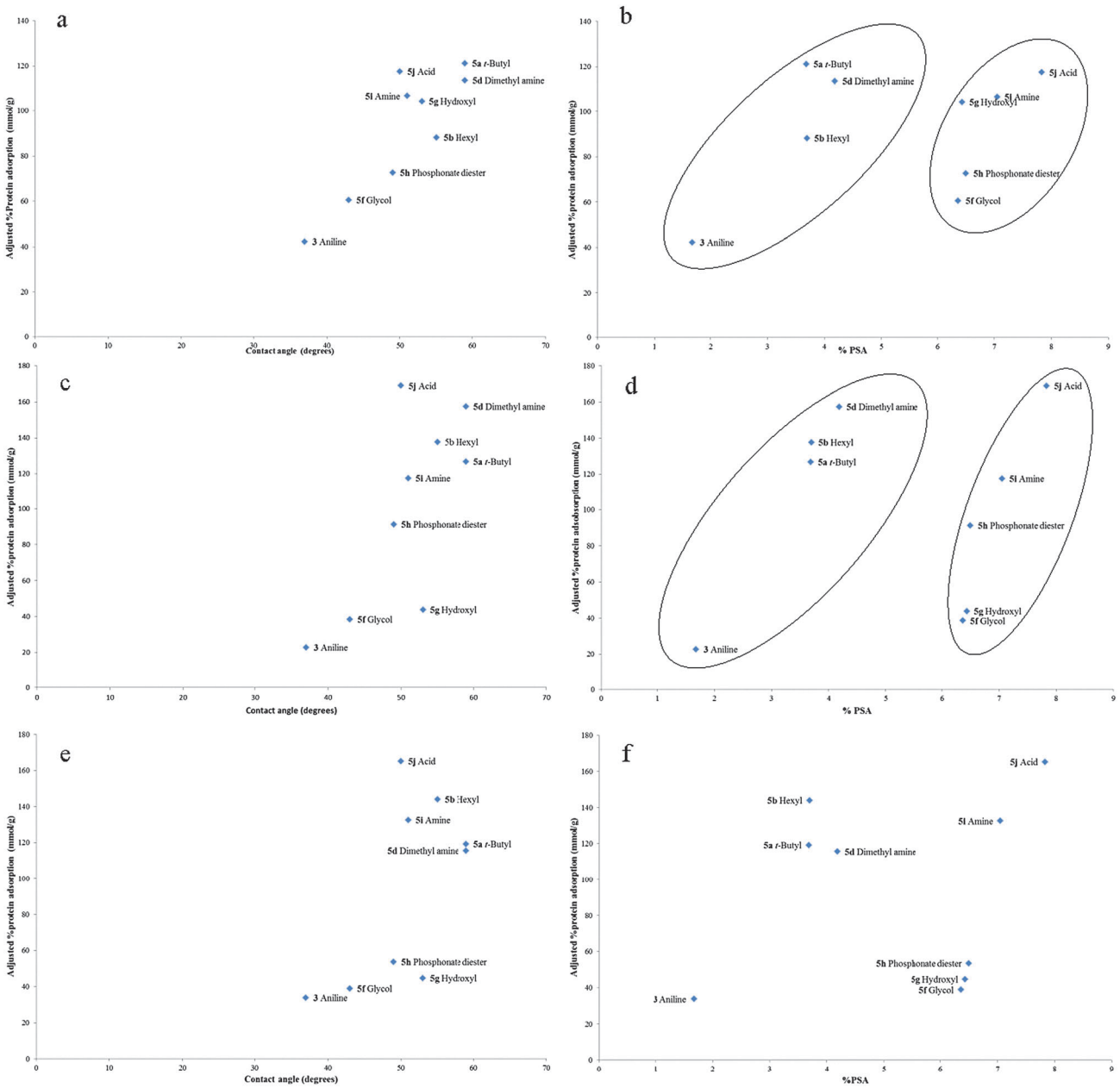

Fig. 6 Protein adsorption with various parameters at different time points. (a) Protein binding with contact angle at 1 h; (b) protein binding with %PSA at 1 h; (c) protein binding with contact angle at 12 h; (d) protein binding with %PSA at 12 h; (e) protein binding with contact angle at 24 h; (f) protein binding with %PSA at 24 h.

(Fig. 6(f)), increased segregation into three groups is observed: phosphonate diester, hydroxyl and glycol comprise one, most likely as a result of water binding to the surface preferentially; hexyl, *tert*-butyl and dimethyl amine form the second as a result of their common van der Waals binding mechanism; and finally the acid and amine due to their greater affinity for the protein or stronger binding ability *via* electrostatic interactions. The data presented here suggest that protein binding may be strongly mediated by surface chemical functionality, with significantly enhanced binding for *tert*-butyl groups **5a**, hexyl **5c**, dimethylamino **5d** and acid **5j** groups relative to the glycol function **5f**, which appears to broadly correlate with %PSA.

Significantly, we have shown that systematic controlled modification of chemical functionality at polymer surfaces is possible, and that this results in changes in macroscopic polymer behaviour such as wettability and protein binding; trends in this behaviour with cheminformatic descriptors of surface functionality can be made. Thus, contact angle and Zeta potential vary with $c \log P$ while an approximate correlation of protein binding with %PSA and contact angle was observed. This surface functionality may be directly responsible for protein binding, or may modify surface hydration leading to a hydrophilic surface layer. These results are of significance, since for example the control of fouling by surface modification has recently been highlighted as a critical element in the design of new materials.[65]

Experimental

Instrumentation and analytical methods

SEM protocol. A scanning electron microscope (JSM6360A, JEOL) was used to observe the surface morphology of microparticles. Dry microparticles were coated with gold and observed microscopically under different magnifications.

Contact angle protocol. For contact angle measurements, the polystyrene microspheres were randomly chosen from each sample group and placed on the surface of a water droplet contained on a clean glass slide. They were imaged using a contact angle analyzer (FTA32 Video 2.0, First Ten Angstroms).[50] Deionized water was used from a Milli-Q system.

Zeta potential protocol. The electrophoretic mobilities of microparticles were measured using a Zeta potential analyzer (Nano-ZS, Malvern Instruments). The particles were suspended in 11% acetone in deionized water at pH 7.18 adjusted using 1 N NaCl and HCl. The electrophoretic mobility was measured at room temperature with 3 runs (12 times in each run) for each sample.

XPS protocol. The surface functionalization of microparticles was analyzed using X-ray photoelectron spectroscopy (XPS) measurements. All XPS spectra were measured using a Kratos Axis Ultra spectrometer with a monochromatic Al–Kα (1486.71 eV) X-ray source. The surface wide scans were recorded with a pass energy of 160 eV and elemental narrow scans were obtained with 40 eV. Casa XPS software was used for curve-fitting analysis of C1s, N1s and O1s with the calibration of binding energy of 284.5 eV for C1s.

TGA analysis. Thermogravimetric analysis (TA Instruments Q2950 and Q500) was used to measure the thermal stability (decomposition temperature (T_d)) of the polystyrene microparticles. Approximately 10 mg of particles were weighed in a platinum TGA pan, which is placed in the high precision balance and heated at a ramp rate of 10 °C per minute over a temperature range of 600 °C in an atmosphere of nitrogen—40% and air—60%.

DSC analysis. DSC thermograms of polystyrene microparticles were obtained using a differential scanning calorimeter (DSC Q10, TA Instruments) to determine the glass transition temperature (T_g). Approximately 5 mg of particles were weighed in an aluminium pan and heated at a ramp rate of 10 or 20 °C per minute over a temperature range of 25 °C to 260 °C in an atmosphere of nitrogen. T_g was calculated using the software by plotting two tangent lines above and below the transition and the temperature midway between the lines was considered as T_g.

Synthetic preparations

(4-((2-(Ethyl(phenyl)amino)ethoxy)methyl)phenyl)(phenyl)-methanone 2a[19]. The following procedure was carried out under an inert atmosphere using dry solvents. A solution of 2-(*N*-ethylanilino)ethanol) (3.32 g, 20.0 mmol) in THF (20 ml) was added to sodium hydride (0.74 g, 31.0 mmol) in THF (5 ml) at −78 °C. The mixture was warmed to room temperature then stirred for 30 minutes and re-cooled to 0 °C. 4-Methylbromobenzophenone[19] (4.95 g, 17.8 mmol) in THF (20 ml) was added, the mixture warmed to room temperature and then left to stir for 72 hours. The THF was removed *in vacuo,* and the reaction quenched with sat. sodium hydrogen carbonate (20 ml). The resulting mixture was washed with DCM (15 ml), and the organic phase was washed with water (2 × 20 ml) then dried over $MgSO_4$, filtered and concentrated to a dark green oil (8.32 g). Purification *via* column chromatography (SiO_2, eluent 9 : 1 petrol (40–60):EtOAc) gave product **2a** as a yellow oil (4.59 g, 72%). R_f 0.45 in 6 : 1 petrol (40–60):EtOAc; ν_{max}(film)/cm^{-1} 2970 (N–H), 1820, 1650, 1625; δ_H (400.2 MHz; $CDCl_3$) 1.21 (3H, t, *J* 7.1, NCH_2CH_3), 3.48 (2H, q, *J* 7.1, NCH_2CH_3); 3.61 (2H, t, *J* 6.2, OCH_2CH_2N), 3.73 (2H, t, *J* 6.2, OCH_2CH_2N), 4.65 (2H, s, $ArCH_2O$), 6.73 (3H, m, ArC*H* 2 × *ortho* and 1 × *para* to NEt), 7.26 (2H, t, *J* 8.0, ArC*H meta* to NEt), 7.46–7.53 (4H, m, 4 × ArC*H meta* to C═O), 7.62 (1H, dd, *J* 7.4, 7.4, ArC*H para* to C═O), 7.83 (4H, d, *J* 7.3, 4 × ArC*H ortho* to C═O); δ_C (100.6 MHz; $CDCl_3$) 12.2 (NCH_2CH_3), 45.5 (NCH_2CH_3), 50.1 (OCH_2CH_3N), 68.5 (OCH_2CH_3N), 72.24 ($ArCH_2O$), 111.8 (2 × ArCH *ortho* to NEt), 115.8 (ArCH *para* to NEt), 127.1, 128.3, 129.4, 130.1 and 130.3 (2 × ArCH *meta* to NEt and 2 × ArCH *meta* to C═O), 136.8 and 137.7 (2 × ArC(C═O)), 143.2 ($ArCCH_2O$), 147.7 (ArCNEt), 196.4 (C═O); *m*/*z* (ESI$^+$) 360.2 ([M + H]$^+$, 100%).

***N*-Ethyl-*N*-(2-((4-(hydrazono(phenyl)methyl)benzyl)oxy)ethyl)-aniline 2b**[19]. Hydrazine monohydrate (2 ml, 4.2 mmol) was added to a solution of (4-((2-(ethyl(phenyl)amino)ethoxy)methyl)-phenyl)(phenyl)methanone **2a** (3.1 g, 8.6 mmol) in EtOH (15 ml) and the mixture was set to reflux. Analysis by mass spectrometry after 16 hours showed complete loss of the benzophenone, so the reaction mixture was cooled to room temperature. Water (5 ml) was added and the EtOH removed *in vacuo*. DCM (10 ml) was added to the residue and the two phases separated. The organic phase was washed with water (3 × 10 ml), dried over $MgSO_4$ and concentrated *in vacuo,* to yield product **2b** as a 1 : 1 mixture of two diastereoisomers as a colourless oil (2.80 g, 87%). ν_{max}(film)/cm^{-1} 3405 br, 2865 br, 1595; δ_H (400.2 M Hz; $CDCl_3$) 1.14–1.22 (3H, m, NCH_2CH_3), 3.40–3.55, 3.59–3.67 and 3.73–3.76 (6H, 3 × m, OCH_2CH_2N and NCH_2CH_3), 4.53 and 4.62 (2H, s, 2 × $ArCH_2$), 5.45 (2H, br s, NH_2), 6.65–6.75 (3H, m, ArC*H*), 7.20–7.32 (7H, m, ArC*H*), 7.46–7.57 (4H, m, ArC*H*); δ_C (100.6 MHz; $CDCl_3$) 12.2 and 12.2 (NCH_2CH_3), 45.4 and 45.5 (NCH_2CH_3), 50.1 (OCH_2CH_2N), 68.0 and 68.4 (OCH_2CH_2N), 73.0 and 73.1 ($ArCH_2O$), 111.7 and 111.8 (2 × ArCH *ortho* to NEt), 115.7 and 115.8 (ArCH *para* to NEt), 126.5, 126.5, 127.4, 128.1, 128.5, 128.8, 128.9, 129.3 and 129.4 (ArCH), 132.2 and 132.9 ($ArCCH_2O$), 137.9, 138.2, 138.4 and 139.2 ($ArCC{=}NNH_2$), 147.7 (ArCNEt), 149.0 and 149.0 (C═N); *m*/*z* (ESI$^+$) 374.2 ([M + H]$^+$, 100%).

***N*-(2-((4-(Diazo(phenyl)methyl)benzyl)oxy)ethyl)-*N*-ethylaniline 2c**. To a stirring solution of *N*-ethyl-*N*-(2-((4-(hydrazono(phenyl)-methyl)benzyl)oxy)ethyl)aniline **2b** (1.04 g, 2.78 mmol) in methanol (34 ml), manganese(IV) oxide (0.61 g, 6.96 mmol), potassium hydroxide (0.16 g, 2.78 mmol) and sodium sulfate (0.56 g, 3.94 mmol) were added. The mixture was stirred for 3 hours when analysis by mass spectrometry showed complete consumption of the starting hydrazone. The methanol was removed *in vacuo,* and DCM was added (30 ml). The mixture was filtered through a Celite plug, and concentrated to give product **2c** as a dark pink oil

(0.91 g, 89%). ν_{max}(film)/cm^{-1} 2865, 2040 (N═N═N), 1660, 1505; δ_H (400.2 MHz; $CDCl_3$) 1.18 (3H, t, *J* 7.0, NCH_2CH_3), 3.45 (2H, q, *J* 7.0, NCH_2CH_3), 3.57 (2H, t, *J* 6.4, OCH_2CH_2N), 3.69 (2H, q, *J* 6.4, OCH_2CH_2N), 4.55 (2H, s, $ArCH_2O$), 6.66–6.73 (3H, m, 2 × ArC*H ortho* to NEt and 1 × ArC*H para* to NEt), 7.19–7.25 (3H, m, 2 × ArC*H meta* to NEt and 1 × ArC*H para* to C–N_2), 7.27–7.32 (4H, m, 4 × ArC*H ortho* to C–N_2), 7.36–7.43 (4H, m, 4 × ArC*H meta* to C–N_2); δ_C (100.6 MHz; $CDCl_3$) 12.2 (NCH_2CH_3), 45.4 (NCH_2CH_3), 50.1 (OCH_2CH_2N), 68.0 (OCH_2CH_2N), 73.0 ($ArCH_2O$), 111.7 (2 × ArCH *ortho* to NEt), 115.7 (ArCH *para* to NEt), 125.2 (ArCH *para* to C–N_2′), 125.6 (2 × ArCH *meta* to NEt), 128.6 and 128.9 (ArCH *ortho* to C–N_2), 129.1 and 129.3 (4 × ArC*H meta* to C–N_2), 129.6 (2 × $ArCCN_2$)), 135.7 (ArCNEt), 147.7 (*C*═N); *m*/*z* (ESI +) 372.2 ([M + H]$^+$, 100%).

Modification of polystyrene XAD-4 beads with *N*-(2-((4-(diazo-(phenyl)methyl)benzyl)oxy)ethyl)-*N*-ethylaniline 2c to give polymer **3**. The supplied XAD-4 beads were washed with copious amounts of water, acetone and then dried. *N*-(2-((4-(Diazo-(phenyl)methyl)benzyl)oxy)ethyl)-*N*-ethylaniline **2c** (5 w/w%, relative to bead weight) was dissolved in ether and the Amberlite XAD-4 beads added. More ether was added such that the beads were completely submerged, and the mixture was carefully concentrated to dryness *in vacuo*. The beads were heated at 120 °C until the beads had turned from pink to off yellow/white colour. The product beads **3** were washed with acetone on a sinter funnel and dried under vacuum.

Diethyl (4-nitrobenzyl)phosphonate.[66] 4-Nitrobenzyl bromide (1.09 g, 5.05 mmol), tetrabutylammonium iodide (132 mg, 0.36 mmol) and triethylphosphite (2 ml, 11.7 mmol) were stirred together at 120 °C for 5 hours. The mixture was cooled and purified by column chromatography on silica (eluent 4 : 1 EtOAc : petrol) to yield a yellow oil (1.07 g, 78%). R_f 0.27 (4 : 1 EtOAc: petrol (40–60)); ν_{max}(neat film)/cm^{-1} 3470, 2985, 1520, 1350, 1250 (P═O), 1025, 965 (P–O); δ_H (400.2 MHz; $CDCl_3$) 1.20 (6H, t, J_{HH} 7.1, 6 × OCH_2CH_3), 3.20 (2H, d, J_{HP} 22.4, 2 × $ArCH_2P$), 3.96–4.03 (4H, m, 4 × OCH_2CH_3), 7.42 (2H, dd, J_{HH} 8.7, J_{HP} 2.3, ArC*H meta* to NO_2), 8.11 (2H, d, J_{HH} 8.7, ArC*H ortho* to NO_2); δ_C (100.6 MHz; $CDCl_3$) 16.3 (d, J_{CP} 6.0, 2 × OCH_2CH_3), 33.8 (d, J_{CP} 136.1, 2 × $ArCH_2P$), 62.4 (d, J_{CP} 7.0, 2 × OCH_2CH_3), 123.6 (d, J_{CP} 3.0, 2 × ArCH *meta* to NO_2), 130.6 (d, J_{CP} 6.0, 2 × ArCH *ortho* to NO_2), 139.7 (d, J_{CP} 9.1, $ArCCH_2P$), 146.9 (d, J_{CP} 4.0, $ArCNO_2$); *m*/*z* (ESI$^-$) 272 ([M–H]$^-$, 100%).

Diethyl (4-aminobenzyl)phosphonate.[67] $SnCl_2{\cdot}2H_2O$ (1.80 g, 7.96 mmol) and HCl (1.2 ml, 39.5 mmol) were added to a stirring solution of diethyl (4-nitrobenzyl)phosphonate (1.07 g, 2.87 mmol) in EtOH (20 ml). The mixture was refluxed for 3.5 hours, cooled to room temperature then the pH adjusted to 8–9 using aq. 5% NaOH solution. The mixture was extracted with DCM (1 × 50 ml, 2 × 20 ml) and the combined organic layers washed with water (20 ml) and brine (20 ml). The organic fraction was dried over $MgSO_4$, and concentrated under vacuum to produce a yellow semi-solid (774 mg). The product was purified through a silica plug using EtOAc to elute the product as a yellow solid (576 mg, 82%). R_f 0.39 (EtOAc); mp 84–85 °C; ν_{max}(DCM film/cm^{-1}) 3430 (N–H), 2980, 1615, 1225 (P═O), 1050, 965, 850; δ_H (400.2 MHz; $CDCl_3$) 1.24 (6H, t, J_{HH} 7.1, 6 × OCH_2CH_3), 3.05 (2H, d, J_{HP} 20.9, 2 × $ArCH_2P(O)$), 3.95–4.05 (4H, m, J_{HH} 7.1, 4 × $P(O)(OCH_2CH_3)_2$), 6.64 (2H, d, J_{HH} 8.4, ArC*H ortho* to NH_2), 7.08 (2H, dd, J_{HH} 8.4, J_{HP} 2.4, ArC*H meta* to NH_2); δ_C (100.6 MHz; $CDCl_3$) 16.4 (d, J_{CP} 6.0, 2 × $P(O)(OCH_2CH_3)_2$), 32.7 (d, J_{CP} 138.8, $CH_2P(O)$), 62.0 (d, J_{CP} 7.0, 2 × $P(O)(OCH_2CH_3)_2$), 115.3 (d, J_{CP} 3.0, ArCH *ortho* to NH_2), 121.0 (d, J_{CP} 10.1, $ArCCH_2$), 130.6 (d, J_{CP} 7.0, ArCH *meta* to NH_2), 145.2 ($ArCNH_2$); *m*/*z* (ESI$^-$) 242.10 ([M–H]$^-$, 100%).

Synthesis and coupling of diazonium salts with modified polymer 3 to give polymers **5a–m**. The diazonium salt (12 w/w%) was prepared based on the mass of the beads to be modified by taking the relevant amine (1 eq.), isopentyl nitrite (1 eq.) (NB: Care! Heart stimulant)* and tetrafluoroboric acid (2 eq.) (NB: in the case of 1,4-phenylenediamine, 1.1 eq. of isopentylnitrite and 2 eq. of tetrafluoroboric acid were used) and by stirring in EtOH at 0 °C for 2 hours. The presence of the desired diazonium salt was confirmed using the H-acid test (see below).[22] The mixture was added to a vial containing the modified beads **3** and EtOH was added such that the beads were completely immersed. The bead salt mixture was left to stand for 18 hours in a fridge at 5 °C. The modified beads **5a–m** were filtered from the mixture, washed with water and EtOH and then left to dry on a sinter funnel under vacuum.

H-acid test. A sample of the diazonium salt solution (1 ml) was adjusted to pH 4 using sodium acetate and then H-acid (4-amino-5-hydroxy-2,7-naphthalene disulfonic acid) was added (10 mg). The mixture was mixed thoroughly and left to stand at room temperature for 15 minutes. The presence of a diazonium salt is indicated by a dark purple colour (Scheme 2). An alternative "spot test" procedure is as follows: drops of the suspension were placed onto a filter paper soaked in 'H-acid' solution. If the diazonium species had been generated, intense colour formation is instantaneous.

Protein adsorption on microparticles

Protein adsorption on microparticles (single time point). Protein adsorption was determined using bovine serum albumin (BSA) with the modified microparticle surfaces. The microparticles were sterilized in methanol for a few minutes, soaked overnight in Dulbecco's Phosphate Buffered Saline (DPBS, Invitrogen), the DPBS was removed and the particles dried in an oven at 37 °C for 24 h. A stock protein solution of BSA in DPBS (5 mg ml^{-1}) was used. Particles (2 mg) were placed in 24 well plates (3 replicates for each sample group) and 1000 μl of BSA solution was added. The plates were then incubated at 37 °C under constant shaking for 3 h and the supernatant was removed, leaving the microparticles with adsorbed protein. Sodium dodecyl sulfate (SDS) solution (1% (w/v), 1 ml) was added to each of the wells and the plates were incubated at 37 °C for 1 h. After 1 h, the SDS solution was removed and optical density (OD) read at a wavelength of 280 nm. The concentration of proteins adsorbed onto the particles was calibrated using a standard curve. The DPBS and BSA without microparticles served as the blank and reference respectively.

Protein adsorption on microparticles (multiple time points). Protein adsorption at different time points was determined using bovine serum albumin (BSA) with the modified microparticle surfaces. The microparticles were sterilized in methanol for

10 min, soaked overnight in DPBS, and dried at 37 °C for 24 h prior to adsorption. A stock protein solution of BSA in DPBS (5 mg ml^{-1}) was used. Each type of modified microparticle was divided into 5 groups (3 replicates) with different incubation times of 1, 3, 6, 12 and 24 h. The microparticles were incubated in 96-well plates, containing microparticles (2 mg) and BSA solution (200 μL) in each well at 37 °C with constant shaking. At every time point, the supernatant was carefully removed from all the samples and transferred to a fresh 96-well plate. The BSA concentration in the supernatant was analyzed spectrophotometrically at 280 nm. The concentration of proteins adsorbed onto the particles can be calculated by subtracting the concentration in the supernatant from 5 mg ml^{-1}, the actual concentration added before incubation.

Acknowledgements

EMP gratefully acknowledges receipt of an industrially funded CASE studentship (Materials KTN and OAS).

References

1 P. Vadgama, *Annu. Rep. Prog. Chem., Sect. C*, 2005, **101**, 14–52.
2 C.-S. Ha and J. A. Gardella, *Chem. Rev.*, 2005, **105**, 4205–4232.
3 D. R. Absolom, W. Zingg and A. W. Neumann, *J. Biomed. Mater. Res.*, 1987, **21**, 161–171.
4 D. E. E. MacDonald, *Biomaterials*, 2002, **23**, 1269–1279.
5 E. Moy, F. Y. H. Lin, J. W. Vogtle, Z. Policova and A. W. Neumann, *Colloid Polym. Sci.*, 1994, **272**, 1245–1251.
6 A. Caro, V. Humblot, C. Methivier, M. Minier, M. Salmain and C.-M. Pradier, *J. Phys. Chem. B*, 2009, **113**, 2101–2109.
7 C.-K. Kang and Y.-S. Lee, *J. Mater. Sci.: Mater. Med.*, 2007, **18**, 1389–1398.
8 B. G. Keselowsky, D. M. Collard and A. J. Garcia, *J. Biomed. Mater. Res.*, 2003, **66**, 247–259.
9 Y. Inoue, T. Nakanishi and K. Ishihara, *React. Funct. Polym.*, 2011, **71**, 350–355.
10 D. R. Schmidt, H. Waldeck and W. J. Kao, in *Biological Interactions on Materials Surfaces*, ed. D. A. Puleo and R. Bizios, Springer, Editon edn, 2009, pp. 1–18.
11 S. J. Dilly, M. P. Beecham, S. P. Brown, John. M. Griffin, A. J. Clark, C. D. Griffin, J. Marshall, Richard. M. Napier, P. C. Taylor and A. Marsh, *Langmuir*, 2006, **22**, 8144–8150.
12 B. Sun, M. Yi, C. C. Yacoob, H. T. Nguyen and H. Shen, *Acta Biomater.*, 2012, **8**, 1109–1116.
13 V. Beachley and X. Wen, *Prog. Polym. Sci.*, 2010, **35**, 868–892.
14 Z. Ma, Z. Mao and C. Gao, *Colloids Surf., B*, 2007, **60**, 137–157.
15 Y. Ikada, *Biomaterials*, 1994, **15**, 725–736.
16 J. M. Goddard and J. H. Hotchkiss, *Prog. Polym. Sci.*, 2007, **32**, 698–725.
17 G. Fourche, *Polym. Eng. Sci.*, 1995, **35**, 968–975.
18 P. J. Davis, L. Harris, A. Karim, A. L. Thompson, M. Gilpin, M. G. Moloney, M. J. Pound and C. Thompson, *Tetrahedron Lett.*, 2011, **52**, 1553–1556.
19 K. Awenat, P. J. Davis, M. G. Moloney and W. Ebenezer, *Chem. Commun.*, 2005, 990–992.
20 H. Wang, J.-P. Griffiths, R. G. Egdell, M. G. Moloney and J. Foord, *Langmuir*, 2008, **24**, 862–868.
21 C. Choong, J.-P. Griffiths, M. G. Moloney, J. Triffitt and D. Swallow, *React. Funct. Polym.*, 2009, **69**, 77–85.
22 J. P. Griffiths, B. Maliha, M. G. Moloney and A. L. Thompson, *Langmuir*, 2010, **26**, 14142–14153.
23 P. Luksirikul, B. Ballesteros, G. Tobias, M. G. Moloney and M. L. H. Green, *Carbon*, 2010, **48**, 1912–1917.
24 M. G. Moloney, *J. Phys. D: Appl. Phys.*, 2008, **41**, 174006.
25 D. Leonard, M. G. Moloney and C. Thompson, *Tetrahedron Lett.*, 2009, **50**, 3499–3502.
26 T. R. Stratton, B. M. Applegate and J. P. Youngblood, *Biomacromolecules*, 2011, **12**, 50–56.
27 K. O. V. Flores, A. P. de Aguiar, M. R. M. P. de Aguiar and L. C. de Santa Maria, *Mater. Lett.*, 2007, **61**, 1190–1196.
28 D. H. Williams and I. Fleming, *Spectroscopic Methods in Organic Chemistry*, McGraw Hill, London, 4 edn. 1987.
29 J. Bernard, C. Branger, T. L. A. Nguyen, R. Denoyel and A. Margaillan, *React. Funct. Polym.*, 2008, **68**, 1362–1370.
30 K. S. Birdi, *Self-Assembly Monolayer Structures of Lipids and Macromolecules at Interfaces*, Springer, 1999.
31 chemicalize.org was used for generating structure property prediction and calculations (http://www.chemicalize.org).
32 See, for example, http://www.emdbiosciences.com/html/NBC/literature.html.
33 J. Rieger, *J. Therm. Anal.*, 1996, **46**, 965–972.
34 J. Anand, S. Palaniappan and D. N. Sathyanarayana, *J. Polym. Sci., Part A: Polym. Chem.*, 1998, **36**, 2291–2299.
35 D. Wang and Y. Liu, *Front. Chem. China*, 2008, **3**, 440–444.
36 M. M. Hann, A. R. Leach and G. Harper, *J. Chem. Inf. Model.*, 2001, **41**, 856–864.
37 K. J. Miller and J. A. Savchik, *J. Am. Chem. Soc.*, 1979, **101**, 7206–7213.
38 A. K. Ghose and G. M. Crippen, *J. Chem. Inf. Model.*, 1987, **27**, 21–35.
39 V. N. Viswanadhan, A. K. Ghose, G. R. Reyankar and R. K. Robins, *J. Chem. Inf. Model.*, 1989, **29**, 163–172.
40 P. Ertl, B. Rohde and P. Selzer, *J. Med. Chem.*, 2000, **43**, 3714–3717.
41 P. Ertl, in *Molecular Drug Properties*, ed. R. Mannhold, Wiley-VCH, Weinheim, 2007, Editon edn, pp. 111–126.
42 P. Ferrara, J. Apostolakis and A. Caflisch, *Proteins: Struct., Funct., Genet.*, 2002, **46**, 24–33.
43 A. Marmur, *Soft Matter*, 2006, **2**, 12–17.
44 I. Meiron and S. Sam, *J. Colloid Interface Sci.*, 2004, **274**, 637–644.
45 D. Y. Y. Kwok, *Langmuir*, 1997, **13**, 2880–2894.
46 T. Yasuda, *Langmuir*, 1994, **10**, 2435–2439.
47 R. J. Good and E. D. Kotsidas, *J. Colloid Interface Sci.*, 1978, **66**, 360–362.
48 Y. Li, J. Q. Pham, K. P. Johnston and P. F. Green, *Langmuir*, 2007, **23**, 9785–9793.
49 K. Holmberg, K. Bergström, C. Brink, E. Österberg, F. Tiberg and J. M. Harris, *J. Adhes. Sci. Technol.*, 1993, **7**, 503–517.
50 G. V. Lubarsky, R. H. Davidson and M. R. Bradley, *Appl. Surf. Sci.*, 2004, **227**, 268–274.
51 A. S. Hoffman, *J. Biomed. Mater. Res.*, 1986, **20**, ix–xi.
52 F. Boury, H. Marchais, J. P. Benoit and J. E. Proust, *Biomaterials*, 1997, **18**, 125–136.
53 G. Yin, Z. Liu, J. Zhan, F. Ding and N. Yuan, *Chem. Eng. J. (Amsterdam, Neth.)*, 2002, **87**, 181–186.
54 G. L. Trainor, *Expert Opin. Drug Discovery*, 2007, **2**, 51–64.
55 G. L. Trainor, in *Annu. Rep. Med. Chem.*, 2007, vol. 42, pp. 489–502.
56 M. P. Gleeson, *J. Med. Chem.*, 2007, **50**, 101–112.
57 P. Ascenzi, A. Bocedi, S. Notari, G. Fanali, R. Fesce and M. Fasano, *Mini-Rev. Med. Chem.*, 2006, **6**, 483–489.
58 J. Ghuman, P. A. Zunszain, I. Petitpas, A. A. Bhattacharya, M. Otagiri and S. Curry, *J. Mol. Biol.*, 2005, **353**, 38–52.
59 P. J. Hajduk, R. Mendoza, A. M. Petros, J. R. Huth, M. Bures, S. W. Fesik and Y. C. Martin, *J. Comput.-Aided Mol. Des.*, 2003, **17**, 93–102.
60 C. M. Stiff, M. Zhong, R. W. Sarver, H. Gao, A. M. Ho, M. T. Sweeney, G. E. Zurenkod and D. L. Romero, *Bioorg. Med. Chem. Lett.*, 2007, **17**, 5479–5482.
61 C. Ybert and J.-M. d. Meglio, *Langmuir*, 1998, **14**, 471–475.
62 N.-P. Huang, R. Michel, J. Voros, M. Textor, R. Hofer, A. Rossi, D. L. Elbert, J. A. Hubbell and N. D. Spencer, *Langmuir*, 2001, **17**, 489–498.
63 H. Noh and E. A. Vogler, *Biomaterials*, 2006, **27**, 5780–5793.
64 H. Noh and E. A. Vogler, *Biomaterials*, 2006, **27**, 5801–5812.
65 D. Rana and T. Matsuura, *Chem. Rev.*, 2010, **110**, 2448–2471.
66 T. Suzuki, O. Nagae, Y. Kato, H. Nakagawa, K. Fukuhara and N. Miyata, *J. Am. Chem. Soc.*, 2005, **127**, 11720–11726.
67 S. Gester, J. Pietzsch and F. Wuest, *J. Labelled Compd. Radiopharm.*, 2007, **50**, 105–113.

